

## The invariant design of planar magnetron sputtering in TFT-LCD

W. J. Yoo, E. Demaray, A. Hosokawa, and R. Pethe

*PVD Research & Development Center, AKT Co., Santa Clara, CA 95054, U.S.A.*

(Received March 12, 1999)

**Abstract** – The main consideration factor to design a magnetron of the sputtering system for TFT-LCD metallization is the high sheet resistance ( $R_s$ ) uniformity which is provided by the high target erosion and high current efficiency. The present study has developed a rectangular magnetron for TFT-LCD to be considered full target erosion and high film uniformity. After an aluminum-2 at.% Nd alloy target was installed in a magnetron source and the film was deposited on the glass of 600×720 mm, the  $R_s$  uniformity of the deposited film was measured as functions of the magnet tilt and magnet scanning configuration. And the target erosion profile was observed with the target voltage. When sputtered at 4 mtorr and 10 kW, the magnet tilt for the high  $R_s$  uniformity of 8.38% was 7 mm. The plasma voltage at the dwell home and end for full-face target erosion, when scanned the magnetron was 120% compared to the mean voltage of the other area.

### I. Introduction

Over the past several years, thin film transistor Liquid crystal displays (TFT-LCD) have replaced the cathode ray tube (CRT). The reason for this replacement is that the use of desktop, personal computers and workstations, full color and multi-scan display capability in TFT-LCD is in great demand [1]. TFT-LCD consists of color filter array, liquid crystal, TFT array and others like backlight and peripheral circuit.

The fabrication of TFT-LCD is performed in three parts: the front glass the preparing color filter, the back glass preparing for the thin film transistor, as well as for metal interconnect lines and the final step which is assembly. When fabricating TFT-LCD's the metallization of TFT, which is used as the gate and pixel signal is one of the important techniques. The sputtering method has been widely used for the metallization of TFT.

The sputtering is defined as the atom ejection process by ion impact and consists of the sputtering source, process chamber, pumping system and controller. Magnetron as a sputtering source is all characterized by nonuniform electric and magnetic fields that are configured to provide the confinement of electrons in the vicinity of the cathode. The electric field is mainly established within the sheath as dark space thickness between the bulk plasma

and the target, while the magnetic field is provided by a set of permanent magnets externally, located behind the target [2-8].

This paper is for investigating the performance and properties of magnetron, which is designed and manufactured to consider the process concept of TFT-LCD metallization. To use the developed magnetron, it is measured the sheet resistance uniformity and investigated the factors affecting the sheet resistance uniformity. In practical usage, a fundamental requirement for TFT-LCD is the uniformity of sheet resistance because the metal line is much longer as the substrate size is increasing. The target erosion region is observed with the target voltage.

### II. Planar magnetron description

#### 2.1. Theory of planar magnetron sputtering

The planar magnetron-sputtering source ejects efficiently the target atoms by the ion impact because the magnetic field is arranged to trap secondary electrons emitted by collisions between electrons and sputtering gases [2, 9-12]. The charged particles show the confinement in front of the sputtering source because the magnetic and electric fields are generated. The equation of motion of these charged particles is as follows [2, 3, 13]

$$m(dV/dt) = q(E + V \times B) \quad (1)$$

where  $q$  is the charged particle,  $E$  is the electric field,  $V$  is the velocity of the charged particle, and  $B$  is the magnetic field strength. In DC magnetron sputtering, there are two first-order equations of motion for charged particles [14, 15]. Electric drift  $V_E$  is

$$V_E = E \times B / B^2 \tag{2}$$

As this equation relates to the helical motion of the charged single particle, it knows that  $V_E$  is independent of  $q$ ,  $m$  and  $v$ . Meanwhile the curvature drift  $V_R$  is

$$V_R = (mv^2/qB)(R_c \times B) / R_c^2 \tag{3}$$

where  $R_c$  is a constant radius of curvature. As this equation relates to the confinement of charged particles, it requires a close path in order to get high charged particle density.

The above Eqs. (2) and (3) are directly proportional to the electric field intensity and inversely proportional to the magnetic field strength. If the magnetic field is decreases or the electric field of the particle is decreased, the electron density to maintain the plasma decreases because it will escape to the confinement easily. So when the magnetron is designed, it should get strong magnet field strength on the target surface.

### 2.2. Magnetron design

The magnetron for TFT-LCD consists of the magnet, target and backing plate, magnet chamber and magnet scan system as shown in Fig. 1. There are several important factors, which must be considered in the magnetron design, as it has high current efficiency, high erosion area and low substrate heating [16].

The first is to get high current efficiency for effective

electron confinement at the high power as the strong magnetic field gets on the target surface as shown in Eqs. (2) and (3). The designed magnetron in this study has been made of the magnet chamber, which gets low pressure for reducing backing plate thickness. It needs to reduce pressure differences between the process chamber and the magnet chamber because they tend to deform inward as result of the pressure difference. As the backing plate thickness reduce, it can get the strong magnetic field on the target surface because the magnetic field in dipole is proportional to  $(r^{-3})$  [17], here  $r$  is the backing plate thickness. Then the magnetron to use TFT-LCD should be rectangular form because of substrate. The magnetron has designed in such a way that the magnet is scanned over the target plate, which is always water flow cooled along with the target to get the full-face target erosion as shown in Fig. 1. Therefore, the magnet scanning configurations and the magnet tilt in a magnetron design for TFT-LCD plays a major role in deciding the uniformity of target erosion and hence uniformity of deposition.

In this study, the magnet was designed as 110 mm by 810 mm to be considered the substrate size of 600 mm×720 mm. Neodymium ferrite barium (NdFeB) as rare-earth alloys was used and the magnetic field was approximately 3500 Gauss. The scan length of the magnet for full-face target erosion is about 780 mm depending on the process conditions. When the magnet is scanning, the electrons, which move toward the close loop in the plasma-ring go out toward the grounded chamber wall as shown in Fig. 2.

Therefore the electrons at both corners escape much more than the other place of magnetron. It can't get good uniformity of plasma and hence uniformity of film because the plasma density of a corner of the magnet is decreased. So, in this study, the

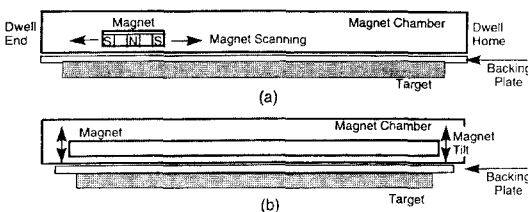


**Fig. 1.** Diagram of planar magnetron for TFT-LCD. (a) Front view, (b) Side view.

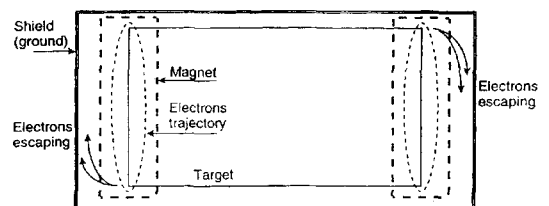


**Fig. 2.** The electrons escaping at the dwell end and home of the magnet configurations.

magnetron was designed to make a tilt in order to control the plasma density of magnetron that it is variable to the magnetic field strength on the target surface. It is efficiently improved the Rs uniformity. In addition, the sputtering source must conduct heat away efficiently because about 80% of the power consumed in plasma generation are lost as heat at the source. In this study, the water cool line at the backing plate controlled the temperature of the target.

### III. Experimental details

Figure 3 shows the schematic diagram of the planar magnetron sputtering system used in this study. As shown in Fig. 3, the planar magnetron sputtering consists of the process chamber including the vacuum system, the magnetron including the magnet chamber, magnet, target and backing plate and the water cool susceptor which controls the temperature of glass as a substrate.

The magnetic field, generated by the permanent magnets, traps the secondary electrons and hence leads to operate in the magnetron mode like high-density plasma, low pressure and high deposition rate. Hence, by adjusting the magnet tilt as shown in Fig. 1, the configuration of the lines of force can be controlled. Figure 4 shows the field mapping at the target surface with 0 to 20 mm of the magnet tilt. The magnet field strength at 20 mm tilt was about 65% compared to the no tilt case. The magnet has been scan to get full-face target erosion and it is important for getting high uniformity to decide the scan configuration of magnet such as the scan time, acceleration and dwell end and home value conditions. In this study, it was investigated relation

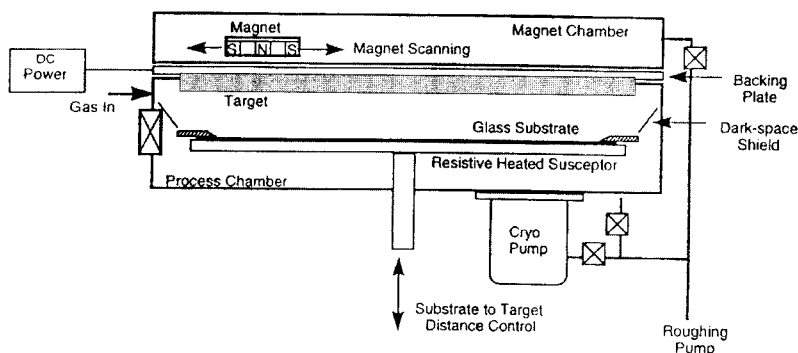


Fig. 3. Schematic diagram of the planar magnetron sputtering system for TFT-LCD used in this experiment.

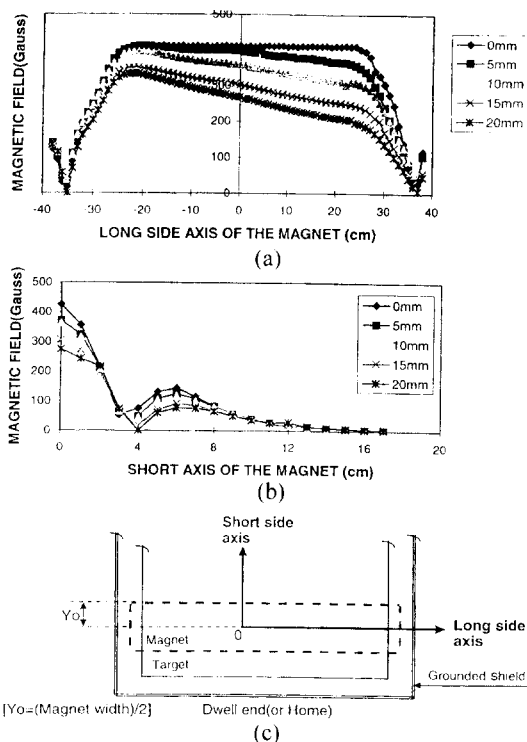


Fig. 4. Mapping of the magnetic field strength on the target surface. (a) long side axis, (b) short side axis, (c) diagram of the measurement axes on the target surface ( $Y_0 = (\text{Magnet width})/2$ ).

among the scan configurations of magnet.

A rectangular form of 890 mm 750 mm to be considered the substrate size and thickness of 8 mm as the aluminum-2 at.% neodymium was used as the target. It was bonded to back plate of aluminum. The table between the target and the substrate can be adjusted 40 to 60 mm and was sputtered at pres-

sure from 2 to 8 mTorr with 200 sccm MFC (mass flow controller). Film deposition was carried out at Ar gas pressure and the process chamber was evacuated to  $3.5 \times 10^{-8}$  Torr by cryo-pump before sputtering and the magnet chamber to 10 Torr. The dc input power is about 18 kW for this system.  $R_s$  (sheet resistance) uniformity of the film is measured by CDE Res Map. The chart recorder measured the target voltage for observation of the target erosion condition. Substrate temperature is measured by a workstation with K type (chromel vs alumel) thermocouple, the so called non-contact thermocouple which is not a contact substrate directly [18].

### IV. Discussion

#### 4.1. Relationship between the gap and the magnet configuration

Figure 5 shows the dwell end and home value in the scan configuration factors of magnets as a function of table, which is between the target and the susceptor distance. In Fig. 5, the table is inversely proportional to the dwell end and home value with percentage maintained at both ends during magnet scanning in order to get high sheet resistance uniformity.

That is the table  $T_h$  is

$$T_h \sim k/D_{e,h}$$

where  $k$  is the constant,  $D_{e,h}$  is the dwell end home value of the magnet-scanning configuration. The reason for this is that the plasma ring and profile affect the table location. The electrons as plasma profile at the dwell end and home value of the magnet scanning goes out toward the susceptor with the table height decreasing.

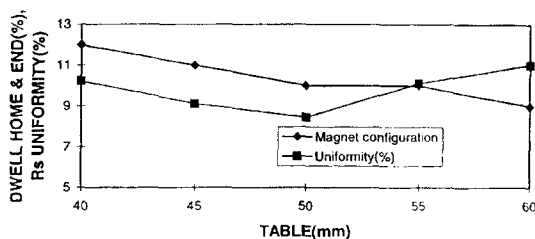


Fig. 5. The dwell home and end value of the magnet configuration and the  $R_s$  uniformity as a function of the table.

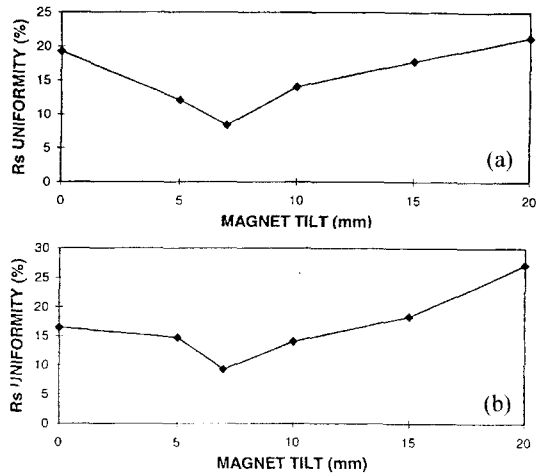


Fig. 6.  $R_s$  uniformity as a function of the magnet tilt at the pressure of 4 mTorr, the table of 50 mm and the power of (a) 10 kW, (b) 15 kW.

#### 4.2. The uniformity of sheet resistance

The  $R_s$  (sheet resistance) uniformity was measured with the magnet tilt. The optimum tilt to get high uniformity, when sputtered at 4 mTorr with an applied power of 10 kW, was 7 mm tilt with 8.38%, with the 10 mm edge exclusion of the substrate and 100 points measurements as shown in Fig. 6. The reason for this is that the electrons, which are confined by a closed magnetic field and rotated clockwise by the curvature drift of Eq. (3) go out toward the chamber wall at the left corner of the dwell end

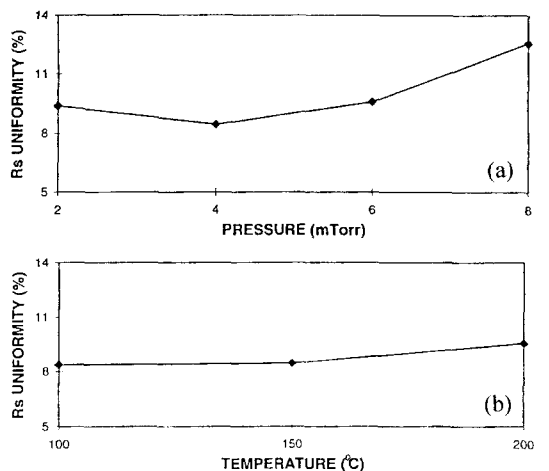


Fig. 7.  $R_s$  uniformity as a function of the pressure (a) and temperature (b).

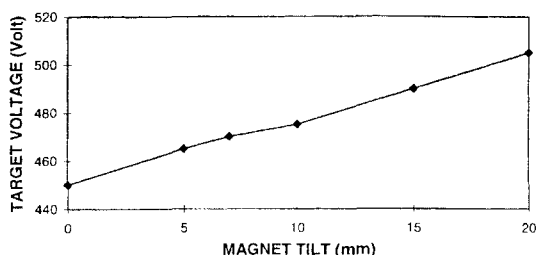


Fig. 8. Target voltage with the magnet tilt.

and home compared to others during the magnet scanning as shown in Fig. 2.

Therefore the electron density is lower at both corners and becomes nonuniform at the dwell end and home value, and hence it can't get high film uniformity. In this study, to make a magnet tilt, which is down the magnet at both corners, can control the electron density on the target surface. Therefore the electron density at the dwell end and home of the magnet assembly scanning can get high uniformity, and hence the  $R_s$  uniformity gets good uniformity. Figure 7 shows the  $R_s$  uniformity as functions of pressure and temperature with a power of 10 kW and a table of 50 mm. It knows that  $R_s$  uniformity depends on pressure but not temperature. The reason is that the plasma sheath and the plasma ring confined by magnetron are changed as a function of the pressure. The pressure influences the ionizability of the plasma in the chamber and determines the relative mean free path of charged particles and sputtered atoms. Therefore the plasma density at the dwell home and end is down by the increase of plasma ring with the pressure decreased because the electrons escape toward the grounded chamber wall faster than the pressure increase case at the normal magnet scan length. But even through the temperature increases, there is no effect to be transferred heat energy to atom mobility on the substrate, which is formed the deposited film and to charged particles.

#### 4.3. Target voltage

The dwell end and home voltage of the magnet configuration for full face target erosion as a function of target voltage, when scanned the magnet, was approximately 120% comparing to the mean voltage of the other area:

$$V_{e,h} = 1.0V_0 + 0.2 V_{ot}$$

where  $V_{e,h}$  is the end and home voltage and  $V_0$  is the mean target voltage. Figure 8 shows the target voltage as a function of the magnet tilt. It knows the voltage increased with the magnet tilt due to the trend of diode sputtering. The average magnetic field strength decreased with the tilt as shown in Fig. 4.

## V. Conclusions

The magnetron to be considered for the process concept of TFT-LCD metallization has been designed and manufactured. To use the manufactured magnetron, it has been investigated in relation between the magnet configuration and the table and measured the  $R_s$  uniformity with the magnet tilt and the target voltage as functions of the magnet tilt, pressure and temperature. The target erosion profile has been investigated with target voltage. The dwell end and home value related the magnet configuration was inversely proportional to the table between the target and the susceptor distance. The magnet tilt for getting high  $R_s$  uniformity of 8.38% at the substrate glass of 600×720 mm was 7 mm. It knows that the  $R_s$  uniformity depended on the pressure but not the temperature. The voltage for full-face target erosion was 120% compared to the scan mean voltage of the other area.

## Acknowledgments

The authors would like to thank R. Mullapui and M. Starr for their assistance in the experiments and all the people in AKT PVD group for all the many useful discussions.

## Reference

- [1] W. E. Howard, *Flat panel Display Technologies*, Japan Display **89**, 1989, pp. 8-11.
- [2] B. Chapman, *Glow Discharge Processes* (John Wiley & Sons, Inc, 1980), p. 177.
- [3] J. A. Thornton, A. S. Penfold and R. K. Waits, in *Thin Film Process*, edited by J. L. Vossen and W. Kern (Academic, New York, 1978), p. 76, p. 131.
- [4] R. P. Howson, A. G. Spenser, K. Oka and R. W. Lewin, *J. Vac. Sci. Technol.* **7**, 1230 (1989).
- [5] Qihua Fan, Xiaohong Chen, Hongyou Chen and Yuan Hong, *J. Vac. Sci. Technol.* **11**, 1230 (1993).
- [6] A. A. Voelodin, P. Stevenson, C. Rebolz, J. M. Schneider and A. Matthews, *Vacuum* **46**, 723 (1995).

- [7] Huai-Wu, Zhang and S. Q. Yang, *Vacuum* **46**, 661 (1995).
- [8] J. Musil, S. Kadlec and W. D. Munz, *J. Vac. Sci. Technol.* **9**, 1171 (1991).
- [9] S. M. Rosnagel and H. R. Kaufman, *J. Vac. Sci. Technol.* **5**, 88 (1987).
- [10] Tatsuo Fukami and Toshiyuki Sakuma, *Jpn. J. Appl. Phys.* **21**, 1680 (1982).
- [11] B. Window and G. L. Harding, *J. Vac. Sci. Technol.* **8**, 1277 (1990).
- [12] F. A. Green and B. N. Chapman, *J. Vac. Sci. Technol.* **13**, 165 (1976).
- [13] T. E. Sheridan, M. J. Goedkner, and j. Goree, *J. Vac. Sci. Technol.* **8**, 30 (1990).
- [14] Russell J. Hill, *Physical Vapor Deposition* 2<sup>nd</sup> ed. (The BOC Group.Inc.), p. 122.
- [15] F. F. Chen, in *Introduction to Plasma Physics* (Plenum, New York, 1974), pp. 2-41.
- [16] G. Mohan, Rao and S. Mohan, *J. Vac. Sci. Technol.* **9**, 3100 (1991).
- [17] D. J. Griffiths, *Introduction to Electrodynamics* 2<sup>nd</sup> ed. ( Prentice Hall, Inc., 1989), p. 234.
- [18] A. Hosokawa. US Patent No. 5,106,200.